

Case report

Two cases of primary diffuse large B-cell lymphoma of the CNS associated with t(8;14)(q24;q32) or t(3;14)(q27;q32) identified by G-banding and fluorescence *in situ* hybridization applied to metaphase spreads

Hitoshi Ohno,^{1,2)} Fumiyo Maekawa,¹⁾ Misumi Nakagawa,¹⁾ Yoshinari Chagi,¹⁾ Miho Nakagawa,¹⁾ Chiyuki Kishimori,¹⁾ Katsuhiro Fukutsuka,¹⁾ Masahiko Hayashida,¹⁾ Kayo Takeoka,¹⁾ Wataru Maruyama,²⁾ Naoya Ukyo,²⁾ Shinji Sumiyoshi³⁾

We describe two patients with primary diffuse large B-cell lymphoma of the central nervous system (PCNS-DLBCL). The first patient (case 1) was a woman in her late 70s who presented with a tumor in the left frontal lobe, whereas the second patient (case 2) was a man in his early 70s who presented with a left frontal lobe tumor associated with intratumoral hemorrhage. The histopathology of the tumor specimen disclosed the proliferation of large cells with centroblastic (case 1) or immunoblastic/plasmablastic (case 2) cytomorphology and an accumulation of the tumor cells within the perivascular space. The cells in both cases were positive for CD20, CD79a, BCL6, IRF4/MUM1, MYC, and BCL2 and negative for CD5 and CD10. G-banding revealed t(8;14)(q24;q32) in case 1, and the tetraploid-range karyotype including two or three copies of der(3)t(3;14)(q27;q32) and der(14)t(3;14)(q27;q32) in case 2. Fluorescence *in situ* hybridization applied to metaphase spreads confirmed colocalization of MYC and IGH (case 1) and BCL6 and IGH (case 2) hybridization signals on the relevant derivative chromosomes. Case 1 carried the MYD88^{L265P} mutation. This case report provides clear evidence for the occurrence of t(8;14)(q24;q32) and t(3;14)(q27;q32) in PCNS-DLBCL using metaphase-based cytogenetic analysis.

Keywords: primary diffuse large B-cell lymphoma of CNS, G-banding, FISH, t(8;14)(q24;q32), t(3;14)(q27;q32)

INTRODUCTION


Because the vast majority of malignant lymphomas that primarily develop in the central nervous system (CNS) exhibit features of diffuse large B-cell lymphoma (DLBCL), the WHO 2017 Classification of Tumours of Haematopoietic and Lymphoid Tissues listed primary DLBCL of CNS (PCNS-DLBCL) as a distinctive category.^{1,2} Tumor cells tend to infiltrate along the perivascular space within the brain, and dissemination to extra-CNS sites is very rare.¹ Treatment consists of high-dose methotrexate-based chemotherapy with or without whole-brain radiotherapy (WBRT), and only in Japan, a novel Bruton's tyrosine kinase inhibitor, tirabrutinib, has been approved for relapsed/refractory cases.³ However, the outcomes remain inferior when compared with other forms of DLBCL.

Characterization of the genomic landscape of PCNS-DLBCL has shown marked progress, including recurrent mutations in JAK-STAT, NF-κB, and the B-cell signaling pathways as well as translocations involving the immunoglobulin (*IG*) genes or non-*IG* loci.^{4,5} In contrast, standard banding analysis of chromosomes has provided very little information on genetic events involved in the development of PCNSL, because of the scarcity of viable tumor cells from brain tissue biopsies or the difficulty in obtaining metaphase cells adequate for banding analysis after the short-term cell culture of tumor cells.⁶ In this study, we performed conventional chromosome preparations from tumor materials in two PCNS-DLBCL cases and obtained metaphase cells adequate for cytogenetic analysis. The results of G-banding and fluorescence *in situ* hybridization (FISH) applied to the metaphase spreads are described.

Received: June 29, 2022. Revised: July 17, 2022. Accepted: August 10, 2022. J-STAGE Advance Published: November 28, 2022
DOI:10.3960/jslrt.22019

¹⁾Tenri Institute of Medical Research, Tenri Hospital, Tenri, Nara, Japan, ²⁾Department of Hematology, Tenri Hospital, Tenri, Nara, Japan, ³⁾Department of Diagnostic Pathology, Tenri Hospital, Tenri, Nara, Japan

Corresponding author: Hitoshi Ohno, MD, PhD, Tenri Institute of Medical Research, Tenri Hospital, 200 Mishima, Tenri, Nara 632-8552, Japan. E-mail: hohno@tenriyoro.zu.jp
Copyright © 2022 The Japanese Society for Lymphoreticular Tissue Research

 This work is licensed under a Creative Commons Attribution-NonCommercial-ShareAlike 4.0 International License.

CASE PRESENTATION

Case 1

A woman in her late 70s presented with constructional apraxia and aphasia associated with right hemiparesis. Magnetic resonance imaging (MRI) of the brain detected a contrast-enhancing tumor in the left frontal lobe extending from the cerebral cortex to the genu of the corpus callosum (Figure 1a and b). The tumor exhibited high intensity on diffusion-weighted imaging (DWI) (Figure 1c) and low intensity in apparent diffusion coefficient (ADC) maps. T2-weighted fluid attenuated inversion recovery (FLAIR) images revealed marked surrounding edema (Figure 1d). The left lateral ventricle was compressed, and a cingulate hernia was found. Her hemoglobin level was 9.1 g/dL, lactate dehydrogenase was 181 U/L, albumin was 3.7 g/dL, and soluble interleukin-2 receptor was 641 U/mL (reference range, 122 to 496 U/mL). She was seronegative for human immunodeficiency virus (HIV).

She underwent a mini-craniotomy and a small part of the tumor was resected, demonstrating DLBCL. ¹⁸F-fluorodeoxyglucose-positron emission tomography combined with computed tomography (CT) confirmed accumulation of the tracer within the brain tumor and the absence of extracranial lesions. The bone marrow was composed of normal hematopoietic precursors. She was treated with a total of 7 cycles of high-dose methotrexate, vincristine, and procarbazine in combination with rituximab (R-MVP) and is currently free from relapse one year and ten months after the initial presentation.

Case 2

A man in his early 70s presented to another hospital with consciousness disturbance and left hemiparesis. Two months earlier, his family noticed that he had become slow, and movement of his upper left limb was awkward. CT of the brain disclosed a hematoma in the right basal ganglia and a tumor in the right frontal lobe (Figure 1e), and he was transferred to our institution. On examination, he was responsive to verbal stimuli. MRI confirmed a contrast-enhancing tumor in the right frontal lobe that extended to the genu of the corpus callosum and was associated with intratumoral hemorrhage (Figure 1f). A small tumor was also found beneath the cerebral cortex in the left frontal lobe. The tumor exhibited increased signal intensity on DWI and reduced ADC values (Figure 1g and h). The midline shifted leftward and intraventricular hemorrhage was noted.

The patient underwent emergent craniotomy for resection of the tumor and hematoma. The histopathology of the excised specimen disclosed DLBCL, and he was then referred to the Hematology Department. A lymphoma staging work-up revealed no sign of systemic disease and the bone marrow was negative. His hemoglobin level was 10.0 g/dL, lactate dehydrogenase was 322 U/L, albumin was 2.9 g/dL, and soluble interleukin-2 receptor was 333 U/mL. Anti-HIV antibody was negative. He was treated with R-MVP and high-dose cytarabine followed by high-dose chemotherapy with autologous hematopoietic support. However, he relapsed soon after and became refractory to tirabrutinib and WBRT. He died 10 months after the initial presentation.

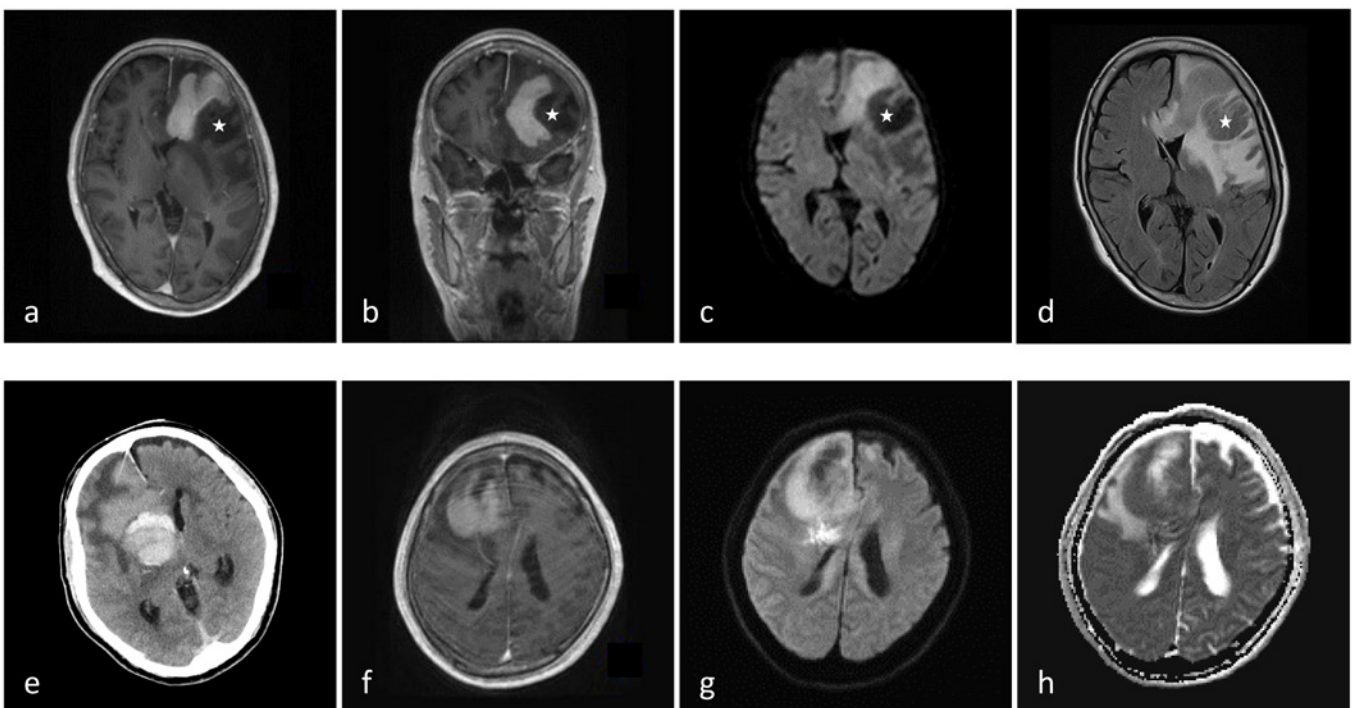


Fig. 1. Imaging studies of PCNS-DLBCL. (a to d) MRI of case 1. Transverse (a) and coronal (b) sections of contrast-enhanced T1-weighted images; DWI (c); and T2 FLAIR image (d). The circular area indicated by asterisks was considered to represent necrotic tissues. (e to h) CT and MRI of case 2. Contrast-enhanced CT image (e); contrast-enhanced T1-weighted MRI (f); DWI (g); and ADC image (h).

EXAMINATION OF TUMOR SPECIMENS

The excised tumor specimen of case 1 showed the proliferation of large cells with dispersed chromatin and nucleoli, representing the centroblastic morphology. The cells accumulated within the perivascular space and, in some areas, were admixed with tingible body macrophages, creating a starry-sky appearance (Figure 2). The lymphoma cells in case 2 showed immunoblastic/plasmablastic cytomorphology with eccentric nuclei and single, central, prominent nucleoli. Perivascular cuffing was prominent (Figure 3). The cells of both cases were positive for CD20, CD79a, BCL6, IRF4/MUM1, MYC, and BCL2 and negative for CD5 and CD10 (Figures 2 and 3). CD138 was negative in case 2. *In situ* hybridization for Epstein-Barr virus-encoded RNA was negative in both cases. The Ki-67 proliferation index was 90%.

Flowcytometry confirmed the expression of B-cell-associated antigens in both cases and monotypic surface immunoglobulins: IgM/ κ in case 1 and IgM/ λ in case 2. CD38 and HLA-DR were positive. The DNA index was 1.00 in case 1 and 2.10 in case 2 compared with normal diploid cells.

CYTOGENETIC AND DNA STUDIES

Lymphoma cells were aseptically prepared from the excised specimens and incubated overnight in RPMI 1640 medium supplemented with 15% heat-inactivated fetal bovine serum at 37°C under a CO₂ concentration of 5%. The cells were then cultured in the presence of 0.1 μ g/mL colcemid for 2 hr. After harvesting, the cells were treated with hypotonic solution and fixed in methanol:acetic acid (3:1). Chromosomes were banded by trypsin-Giemsa staining and the results of the chromosome analysis were described according to the ISCN 2020.

G-banding of metaphase spreads in case 1 revealed t(8;14)(q24;q32) in addition to +7 and additional chromosomal materials of chromosomes 3, 4, 10, and 12; the last led to partial trisomy of 1q (Figure 4A). FISH using *MYC* and *IGH* break-apart (BA) probes demonstrated that der(8) was labeled by the centromeric 5' *MYC* and telomeric 5' *IGH* probes and der(14) was labeled by the telomeric 3' *MYC* and centromeric 3' *IGH* probes, respectively, confirming t(8;14)(q24;q32)/*MYC*::*IGH* translocation (Figure 4B). Accordingly, interphase nuclei hybridized with the *MYC-IGH* dual fusion (DF) probe exhibited the one red, one green, and

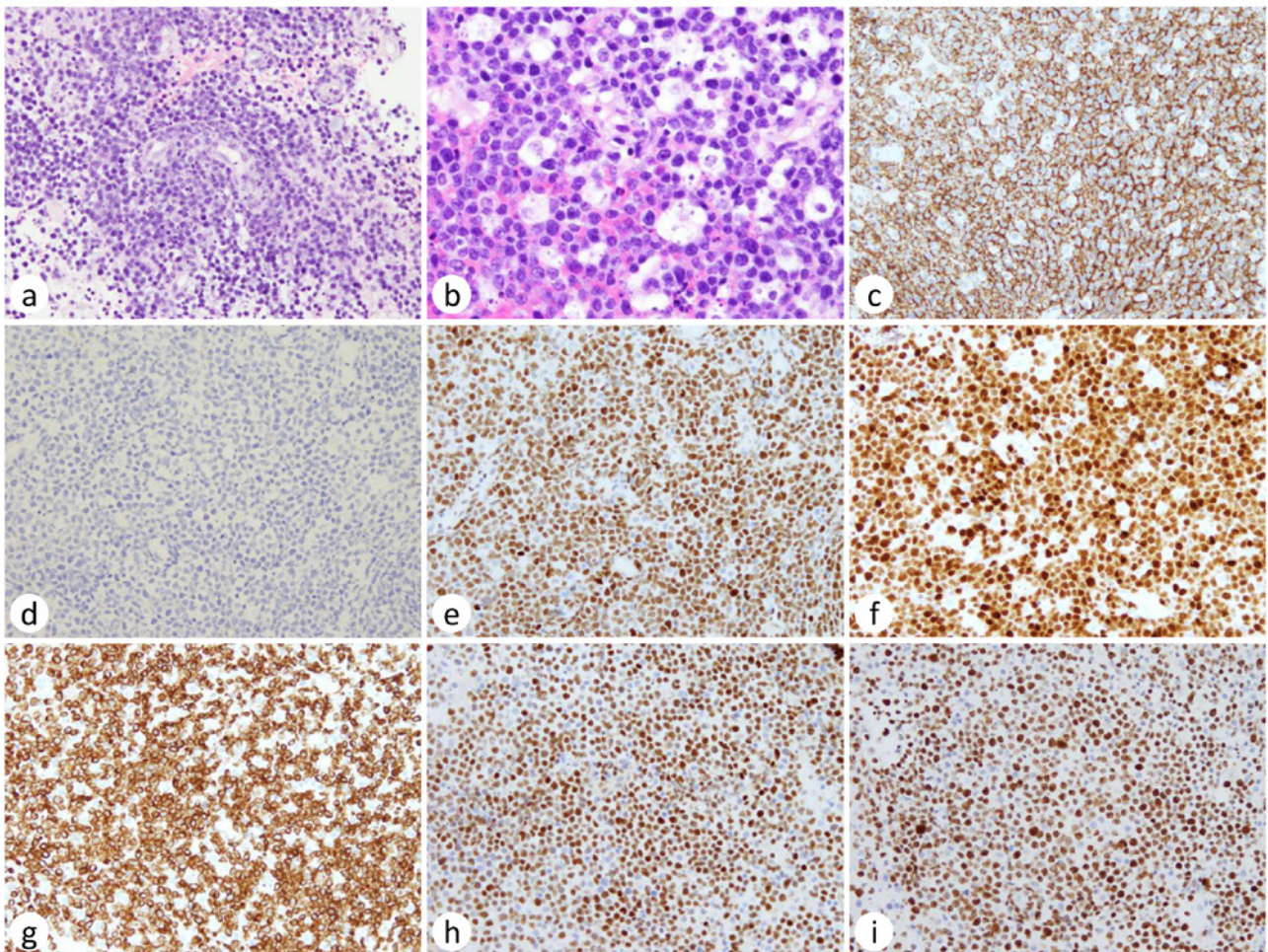


Fig. 2. Histopathology of PCNS-DLBCL in case 1. *a*, hematoxylin & eosin (H&E) staining (original magnification of objective lens, 20 \times); *b*, H&E (40 \times); *c*, anti-CD20 immunostaining (20 \times); *d*, anti-CD10 (20 \times); *e*, anti-BCL6 (20 \times); *f*, anti-IRF4/MUM1 (20 \times); *g*, anti-BCL2 (20 \times); *h*, anti-MYC (20 \times); and *i*, anti-Ki-67 (20 \times).

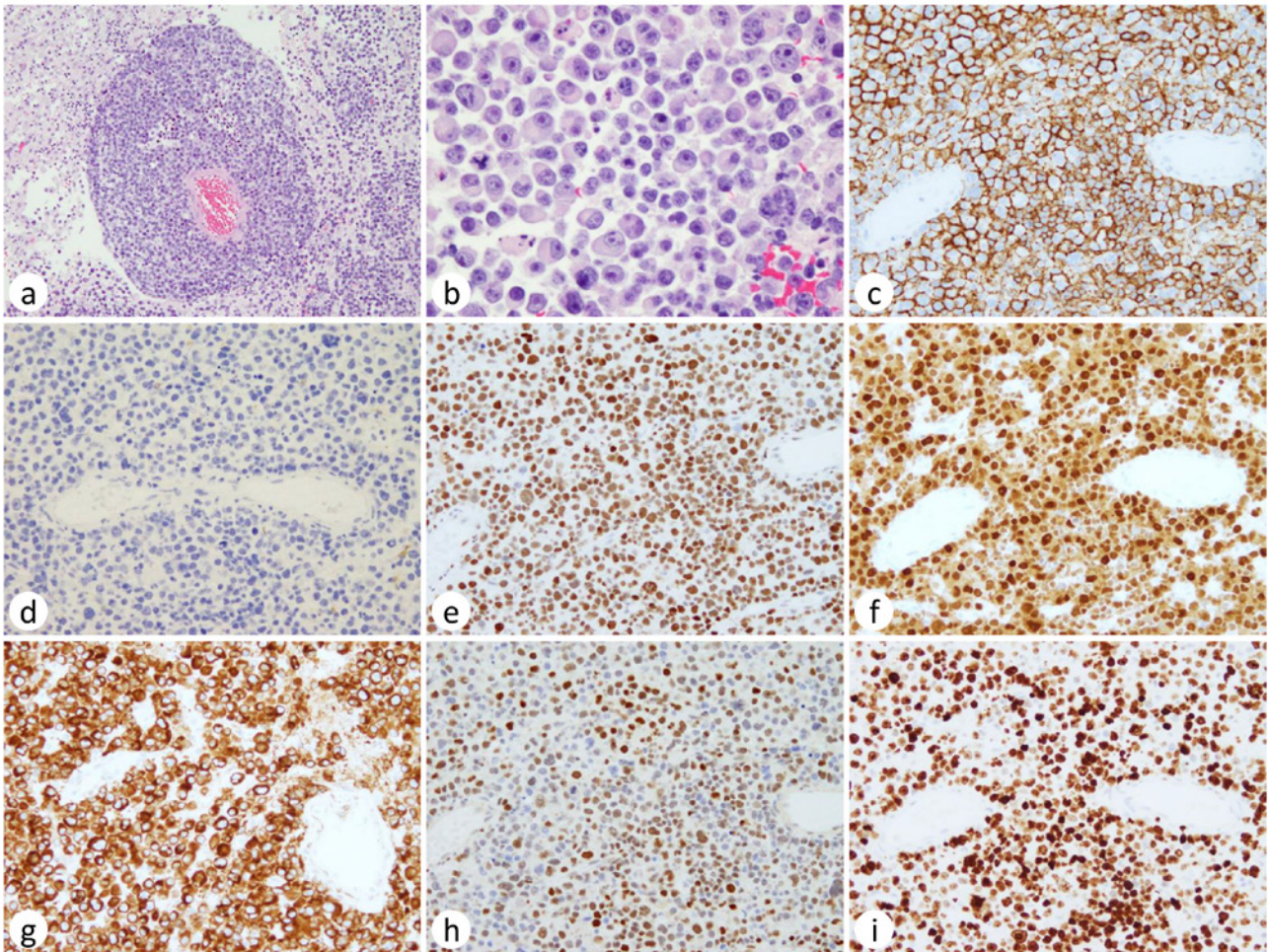


Fig. 3. Histopathology of PCNS-DLBCL in case 2. *a*, H&E staining (10 \times); *b*, H&E (40 \times); *c*, anti-CD20 immunostaining (20 \times); *d*, anti-CD10 (20 \times); *e*, anti-BCL6 (20 \times); *f*, anti-IRF4/MUM1 (20 \times); *g*, anti-BCL2 (20 \times); *h*, anti-MYC (20 \times); and *i*, anti-Ki-67 (20 \times).

two fusion (yellow) signal pattern (not shown). The karyotype according to ISCN was 47,XX,add(3)(p21),add(4)(q35),+7,t(8;14)(q24;q32),add(10)(p13),der(12)t(1;12)(q21;q24).ish t(8;14)(3'MYC-,5'IGH+;5'IGH-,3'MYC+).

G-banding of case 2 revealed near-tetraploid karyotypes including two or three copies of der(3)t(3;14)(q27;q32) and der(14)t(3;14)(q27;q32) (Figure 5A). Additional abnormalities included del(6)(q2?) and two copies of del(17)(p11.2), and structural abnormalities involving chromosomes 1, 2, 5, and 19, and unknown markers were found. FISH using *BCL6* and *IGH* BA probes confirmed colocalization of the centromeric 3' *BCL6* and telomeric 5' *IGH* probes on der(3) and the telomeric 5' *BCL6* and centromeric 3' *IGH* probes on der(14), respectively (Figure 5B). Two marker chromosome homologues were labeled by the unarranged *BCL6* probes at the telomeric ends. FISH using *MYC* and *BCL2* probes demonstrated increased copies of hybridization signals in accordance with the polyploidy, but no BA signals were found (Figure 5C).

Long-distance polymerase chain reaction (LD-PCR) for long targets amplified DNA encompassing the *MYC* exon 2 and *IGHA* in case 1 (Figure 4C) and the 5' sequences of *BCL6* and *IGHM* in case 2 (Figure 5D).⁷ Case 1 carried the *MYD88*^{L265P} mutation (Figure 4D) but lacked the *CD79B*^{Y196}

mutation, and case 2 was negative for both mutations.

DISCUSSION

We described here two cases of PCNS-DLBCL that developed in immunocompetent elderly patients. After the short-term culture of lymphoma cells prepared from tumor tissues, we obtained metaphase spreads adequate for G-banding karyotyping and FISH. The results showed that one case carried t(8;14)(q24;q32) that fused *MYC* to *IGH* and the other case carried t(3;14)(q27;q32) that fused *BCL6* to *IGH*. This case report provides clear evidence for the occurrence of t(8;14) and t(3;14) in PCNS-DLBCL using metaphase-based cytogenetic analysis.

Rearrangements involving the *MYC* gene have been rarely detected in PCNS-DLBCL cases by FISH using the *MYC* BA probe, which is clearly different from extra-CNS DLBCL, where *MYC* rearrangement is observed in approximately 10% of cases.^{8,9} In the largest series of PCNS-DLBCL, 2 (2%) of 108 patients exhibited BA signals, confirming further that the *MYC* rearrangement is uncommon.¹⁰ Accordingly, *MYC*, *BCL2*, and/or *BCL6* double-/triple-hit events are very rare.^{10,11} On the other hand, the presence of t(8;14)(q24;q32)/*MYC*::*IGH* in case 1 raises the possibility

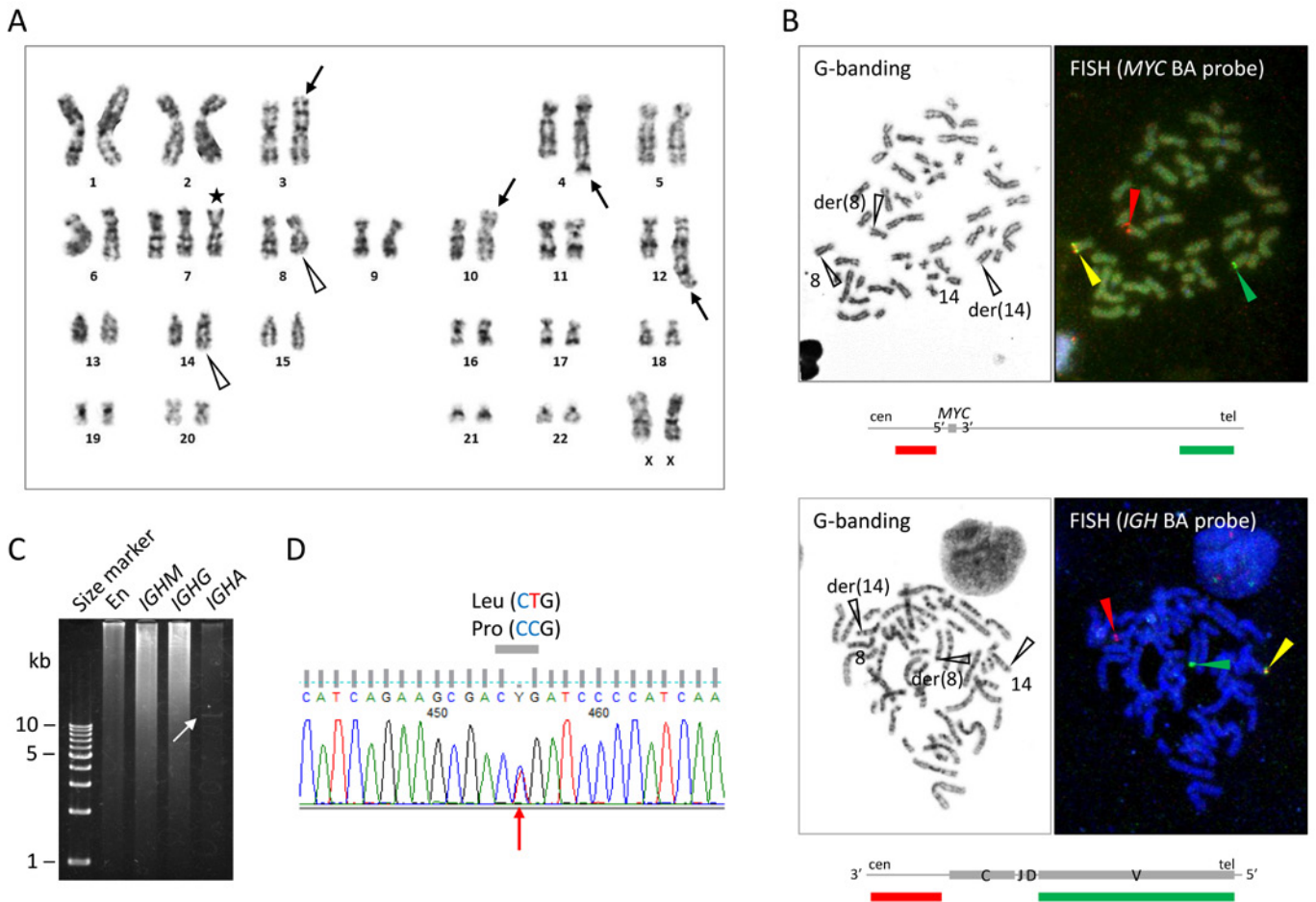


Fig. 4. G-banding, FISH, and DNA tests in case 1. (A) G-banding karyotype. t(8;14)(q24;q32) is indicated by the open arrowheads, and additional structural and numerical abnormalities are indicated by the arrows and asterisk. (B) FISH of metaphase spreads using the *MYC* (top) and *IGH* (bottom) BA probes (Abbott Laboratories, Abbott Park, IL, USA). G-banding and FISH through the triple-band pass filter are aligned side by side. Hybridization signals on the relevant chromosomes are indicated by the arrowheads of their respective colors. Diagrams of the two probes provided by the manufacturer are shown at the bottom. (C) Ethidium bromide (EtBr)-stained gel electrophoresis of LD-PCR products encompassing the t(8;14)(q24;q32)/*MYC::IGH* junction.⁷ The arrow indicates the products amplified by the *MYC* exon 2 and *IGHA* primer combination. (D) Sanger sequencing showing the *MYD88*^{L265P} mutation. The wild-type (thymidine) and mutated (cytosine) alleles represent equivalent electrophoretic peaks (arrow).

that this case represented Burkitt lymphoma (BL) that primarily developed in CNS, i.e., primary CNS BL, which has been sporadically described in the literature;^{12–15} indeed, the biopsy included areas of the starry-sky histopathology, suggesting high-grade B-cell lymphoma. Primary CNS BL occurs in patients of all ages from infants to the elderly and presents with not only brain and spinal cord tumors but also intraventricular tumor growth.¹⁴ Tumors are positive for CD10 and CD20 and negative for BCL2 and show a >99% Ki-67 labelling index.¹⁴ In case 1, in contrast, the lymphoma cells exhibited non-germinal center B-cell/activated B-cell-like immunohistochemistry (IHC) and expressed BCL2 at a high level, indicating that primary CNS BL was unlikely. The presence of *MYD88*^{L265P} mutation supports the diagnosis of PCNS-DLBCL.

BCL6 rearrangements have been observed in 17 to 38% of PCNS-DLBCL cases by FISH using the *BCL6* BA probe applied to tissue sections or single cells,^{2,6,10,11,16–19} and associated with worse progression-free and overall survivals of PCNS-DLBCL patients,^{10,18} potentially accounting for the

poor treatment outcome in case 2. The gene is rearranged with not only *IG* genes but also a variety of non-*IG* genes, resulting from translocations with other chromosomal loci or deletions of upstream sequences, and juxtaposed to the regulatory sequences of each partner gene.^{5,16,17} Rearrangement of *BCL6* with *IGH*, which is the molecular equivalent of t(3;14)(q27;q32), has been demonstrated by the *BCL6-IGH* DF probe in selected cases.^{17,18,20} The translocation occurs between the switch region of *IGHM* and the major translocation cluster of *BCL6*,¹⁷ providing evidence that this translocation is mediated by the class switch recombination and somatic hypermutation mechanism.² Targeted DNA sequencing technology and detection algorithms isolated sequences encompassing the *BCL6::IGH* junction and showed that *BCL6* comes under the control of the super enhancer of *IGH*.⁵ On the other hand, an increase of *BCL6* copies has been identified in association with or without *BCL6* rearrangement.^{6,10} In case 2, we found extra copies of non-rearranged *BCL6* on the two marker chromosome homologues, in addition to t(3;14)(q27;q32), most likely leading to

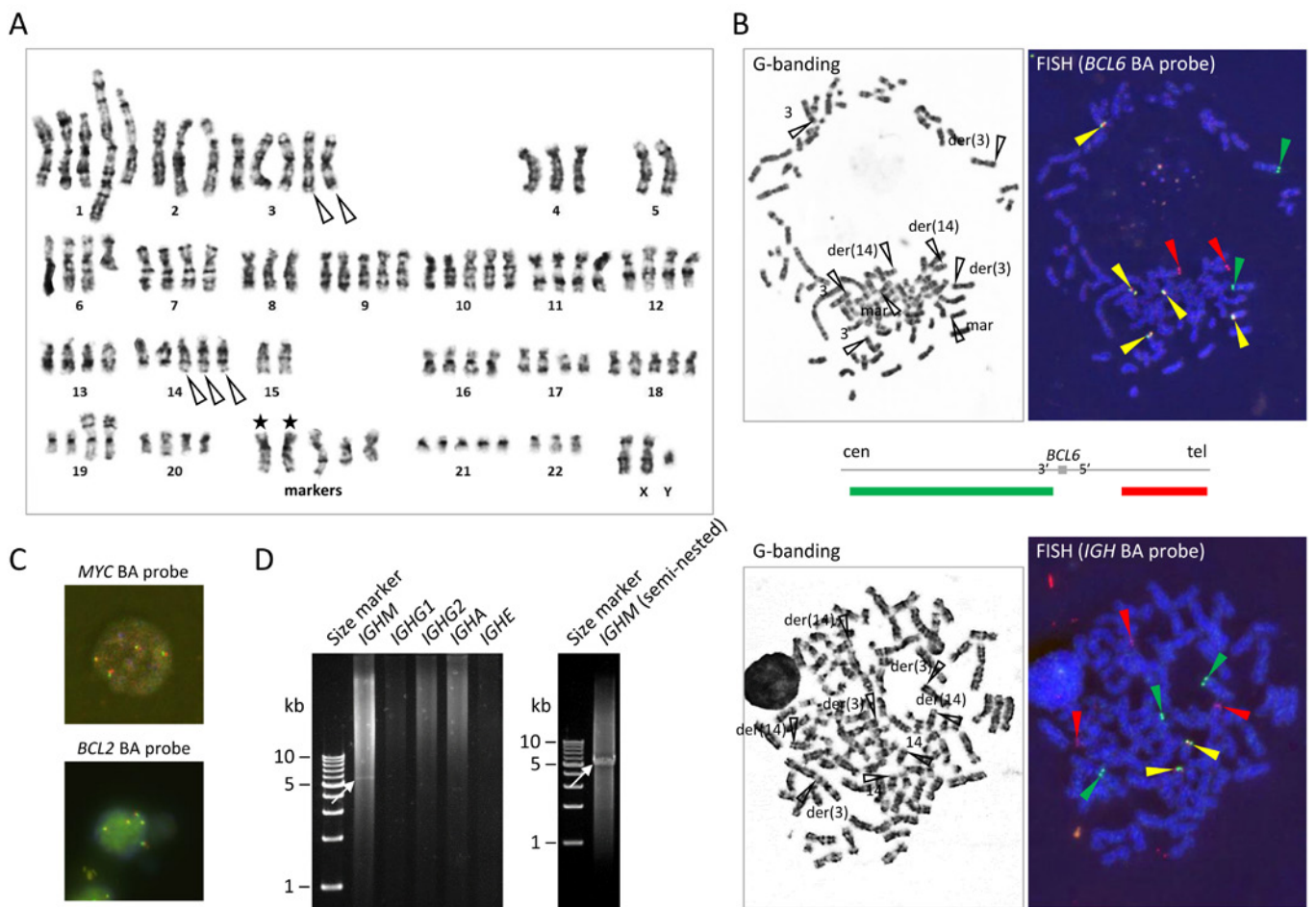


Fig. 5. G-banding, FISH, and DNA tests in case 2. (**A**) G-banding karyotype. Two copies of der(3)t(3;14)(q27;q32) and three copies of der(14)t(3;14)(q27;q32) are indicated by the open arrowheads. The two marker chromosome homologues indicated by the asterisks were labeled by the non-rearranged *BCL6* hybridization signals in **B**. The karyotype may be described as: 95,XXY,-Y,der(1),+der(1),-2,der(2),der(2),+3,t(3;14)(q27;q32)×2,-4,-5,-5,add(5)(p15)×2,del(6q2?),-8,+9,+10,+der(14)t(3;14)(q27;q32),-15,-15,del(17)(p11.2)×2,+18,der(19)add(19)(p13)add(19)(q13)×2,+21,-22,+5mar. (**B**) FISH of metaphase spreads using the *BCL6* (Abbott Laboratories; *top*) and *IGH* (*bottom*) BA probes. G-banding and FISH through the triple-band pass filter are aligned side by side. Hybridization signals on the relevant chromosomes are indicated by the arrowheads of their respective colors. Diagram of the *BCL6* BA probe provided by the manufacturer is shown. (**C**) FISH of interphase nuclei using *MYC* (*top*) and *BCL2* (*bottom*) BA probes (Abbott Laboratories), showing 4 *MYC* and 5 *BCL2* hybridization signals. (**D**) EtBr-stained gel electrophoresis of LD-PCR encompassing the t(3;14)(q27;q32)/*BCL6*::*IGH* junction.⁷ The arrows indicate 1st (*left*) and 2nd (*right*) round PCR products amplified by primers for the 5' sequences of *BCL6* and *IGHM* constant gene. The sequences of the primers used in this study are listed in Supplementary Table S1.

the deregulated and high-level expression of *BCL6* protein. Nevertheless, as the incidence and molecular anatomy of *BCL6* rearrangements are comparable to those in extra-CNS DLBCL, it remains to be determined to what extent the *BCL6* alterations contribute to the pathogenesis of PCNS-DLBCL.

The two cases shared expression of *MYC*, *BCL2*, and *BCL6* and a 90% Ki-67 labeling index in accordance with the general IHC pattern of PCNS-DLBCL.¹ In one series of primary lymphoma of the CNS, *MYC*/*BCL2* double- and *MYC*/*BCL2*/*BCL6* triple-expression were observed in 41 (82%) and 35 (70%) of the 50 cases studied, respectively,²¹ and the higher incidence of the former expression pattern than extra-CNS DLBCL may account for the poor clinical outcome associated with PCNS-DLBCL. Considering the above-discussed incidence of *MYC* and *BCL6* rearrangements and absence of *BCL2* rearrangement in PCNS-DLBCL, the expression of these three proteins may not be attributed to

rearrangements of the corresponding genes. Indeed, it is difficult to find a clear difference of *MYC* and *BCL6* expression by IHC between case 1 (positive for *MYC* rearrangement and negative for *BCL6* rearrangement) and case 2 (negative for *MYC* rearrangement and positive for *BCL6* rearrangement and copy number increase). To elucidate this issue, it is necessary to quantitatively evaluate the expression levels of *MYC* and *BCL6* proteins in PCNS-DLBCL tissues, in parallel with FISH tests.

ACKNOWLEDGMENTS

The authors acknowledge Dr. Shoichi Tani (Department of Neurosurgery, Tenri Hospital) for consultation regarding neurosurgery and Dr. Takeshi Kubo (Department of Radiology, Tenri Hospital) for radiological consultation. This study was supported by Tenri Foundation.

AUTHOR CONTRIBUTIONS

H.O. was responsible for writing the manuscript, literature review, preparing the figures, and overall revision of the manuscript. F.M., M.N., Y.C., M.N., C.K., M.H., K.F., and K.T. were involved in providing data of the cytogenetic and DNA tests and flowcytometric analysis. W.M. and N.U. were involved in the treatment of patients. S.S. was involved in the pathological diagnosis.

ETHICAL APPROVAL

All procedures performed in this study involving the patients were conducted in accordance with the 1964 Helsinki declaration. This study was performed according to the regulations of the Institutional Review Board (Approval No. 1281).

CONSENT FOR PUBLICATION

Appropriate informed consent was taken from the patient (case 1) and the patient's spouse (case 2) for the publication of this manuscript and associated images.

CONFLICT OF INTEREST

The authors declare that they have no conflicts of interest.

REFERENCES

- 1 Kluin PM, Deckert M, Ferry JA. Primary diffuse large B-cell lymphoma of the CNS. In: Swerdlow SH, Campo E, Harris NL, *et al.* (eds): WHO Classification of Tumours of Haematopoietic and Lymphoid Tissues. 4th ed, Lyon, IARC. 2017; pp. 300-302.
- 2 Montesinos-Rongen M, Brunn A, Sanchez-Ruiz M, *et al.* Impact of a faulty germinal center reaction on the pathogenesis of primary diffuse large B cell lymphoma of the central nervous system. *Cancers (Basel)*. 2021; 13: 6334.
- 3 Munakata W, Tobinai K. Tirabrutinib hydrochloride for B-cell lymphomas. *Drugs Today (Barc)*. 2021; 57: 277-289.
- 4 Radke J, Ishaque N, Koll R, *et al.* The genomic and transcriptional landscape of primary central nervous system lymphoma. *Nat Commun*. 2022; 13: 2558.
- 5 Chapuy B, Roemer MGM, Stewart C, *et al.* Targetable genetic features of primary testicular and primary central nervous system lymphomas. *Blood*. 2016; 127: 869-881.
- 6 Montesinos-Rongen M, Zühlke-Jenisch R, Gesk S, *et al.* Interphase cytogenetic analysis of lymphoma-associated chromosomal breakpoints in primary diffuse large B-cell lymphomas of the central nervous system. *J Neuropathol Exp Neurol*. 2002; 61: 926-933.
- 7 Akasaka T, Akasaka H, Ohno H. Polymerase chain reaction amplification of long DNA targets: application to analysis of chromosomal translocations in human B-cell tumors (review). *Int J Oncol*. 1998; 12: 113-121.
- 8 Rosenwald A, Bens S, Advani R, *et al.* Prognostic significance of *MYC* rearrangement and translocation partner in diffuse large B-cell lymphoma: a study by the Lunenburg Lymphoma Biomarker Consortium. *J Clin Oncol*. 2019; 37: 3359-3368.
- 9 Chong LC, Ben-Neriah S, Slack GW, *et al.* High-resolution architecture and partner genes of *MYC* rearrangements in lymphoma with DLBCL morphology. *Blood Adv*. 2018; 2: 2755-2765.
- 10 Villa D, Tan KL, Steidl C, *et al.* Molecular features of a large cohort of primary central nervous system lymphoma using tissue microarray. *Blood Adv*. 2019; 3: 3953-3961.
- 11 Nosrati A, Monabati A, Sadeghipour A, *et al.* *MYC*, *BCL2*, and *BCL6* rearrangements in primary central nervous system lymphoma of large B cell type. *Ann Hematol*. 2019; 98: 169-173.
- 12 Jiang L, Li Z, Finn LE, *et al.* Primary central nervous system B cell lymphoma with features intermediate between diffuse large B cell lymphoma and Burkitt lymphoma. *Int J Clin Exp Pathol*. 2012; 5: 72-76.
- 13 Jiang M, Zhu J, Guan Y, Zou L. Primary central nervous system burkitt lymphoma with non-immunoglobulin heavy chain translocation in right ventricle: case report. *Pediatr Hematol Oncol*. 2011; 28: 454-458.
- 14 Alabdulsalam A, Zaidi SZA, Tailor I, Orz Y, Al-Dandan S. Primary burkitt lymphoma of the fourth ventricle in an immunocompetent young patient. *Case Rep Pathol*. 2014; 2014: 630954.
- 15 Bower K, Shah N. Primary CNS Burkitt lymphoma: a case report of a 55-year-old cerebral palsy patient. *Case Rep Oncol Med*. 2018; 2018: 5869135.
- 16 Montesinos-Rongen M, Akasaka T, Zühlke-Jenisch R, *et al.* Molecular characterization of *BCL6* breakpoints in primary diffuse large B-cell lymphomas of the central nervous system identifies *GAPD* as novel translocation partner. *Brain Pathol*. 2003; 13: 534-538.
- 17 Schwindt H, Akasaka T, Zühlke-Jenisch R, *et al.* Chromosomal translocations fusing the *BCL6* gene to different partner loci are recurrent in primary central nervous system lymphoma and may be associated with aberrant somatic hypermutation or defective class switch recombination. *J Neuropathol Exp Neurol*. 2006; 65: 776-782.
- 18 Cady FM, O'Neill BP, Law ME, *et al.* *Del(6)(q22)* and *BCL6* rearrangements in primary CNS lymphoma are indicators of an aggressive clinical course. *J Clin Oncol*. 2008; 26: 4814-4819.
- 19 Pina-Oviedo S, Bellamy WT, Gokden M. Analysis of primary central nervous system large B-cell lymphoma in the era of high-grade B-cell lymphoma: Detection of two cases with *MYC* and *BCL6* rearrangements in a cohort of 12 cases. *Ann Diagn Pathol*. 2020; 48: 151610.
- 20 Braggio E, Van Wier S, Ojha J, *et al.* Genome-wide analysis uncovers novel recurrent alterations in primary central nervous system lymphomas. *Clin Cancer Res*. 2015; 21: 3986-3994.
- 21 Brunn A, Nagel I, Montesinos-Rongen M, *et al.* Frequent triple-hit expression of *MYC*, *BCL2*, and *BCL6* in primary lymphoma of the central nervous system and absence of a favorable *MYC*^{low}*BCL2*^{low} subgroup may underlie the inferior prognosis as compared to systemic diffuse large B cell lymphomas. *Acta Neuropathol*. 2013; 126: 603-605.